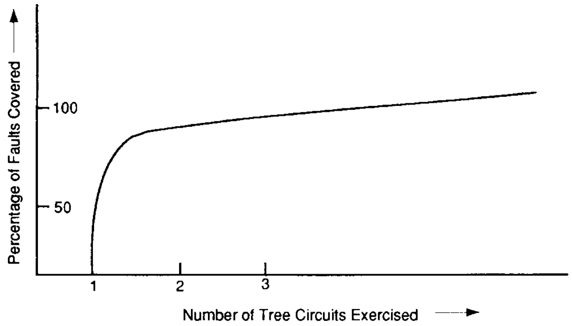

Fig. 8. The relation between $DPLB$ coverage and the number of tree circuits exercised.

have been exercised. If this happens, an improved version of the cutting algorithm can be applied to cover the *tricky* faults [14].

VI. Conclusions

CACOP, a new testability analyses method, has been proposed in this paper. The examples demonstrate that CACOP is quite suitable to derive the lower bounds of the detection probabilities. Most faults can be covered in the first several propagations. The benefits of using CACOP are twofold: 1) CACOP can be used to alleviate the computing complexity of the cutting algorithm without losing the tightness of $DPLB$s; 2) CACOP can be used as a one-sided (i.e., never overestimates detection probabilities) probabilistic testability measuring tool with the aid of the improved cutting algorithm if the computing time is tolerable [14].

In 1984, at the International Test Conference, a panel on *Will Testability Analysis Replace Fault Simulation* concluded with a clear identification of two problems: 1) fault simulation will be too expensive for the million-device chips of the future; and 2) improvements are needed in the testability analyses techniques [13]. Since fault simulation is too expensive, testability analysis is a possible alternative. CACOP is a compromise of $O(n^2)$ and $O(n)$ testability analyses methods from the viewpoint of computing complexity, and the accuracy of detection probability lower bound estimation is potentially better than $O(n^2)$ testability analyses methods.

In future, consideration will be given to select *good* lines to be broken such that most faults can be covered by only a limited number of tree circuits. The bound distortion is significant if the broken lines feed AND gates, and this should preferably be avoided in the tree circuit generation.

Acknowledgment

The authors would like to thank the reviewers for their constructive and helpful suggestions. Thanks are also due to Dr. Jacob Savir for his many useful discussions.

References

[1] P. H. Bardell, W. H. McAnney, and J. Savir, *Built-In Test for VLSI—Pseudorandom Techniques*. New York: Wiley, 1987.
[2] E. J. McCluskey, "Built-in self-test techniques," *IEEE Design & Test of Computers*, vol. 2, pp. 21–28, Apr. 1985.
[3] H. Fujiwara, *Logic Testing and Design for Testability*. Cambridge, MA: MIT Press, 1985.
[4] K. P. Parker and E. J. McCluskey, "Probabilistic treatment of general combinational networks," *IEEE Trans. Computers*, vol. C-24, pp. 668–670, June 1975.
[5] J. Savir, G. S. Ditlow, and P. H. Bardell, "Random pattern testability," *IEEE Trans. Computers*, vol. C-33, pp. 79–90, Jan. 1984.
[6] F. Brglez, "A fast fault grader: Analysis and applications," in *Proc. Int. Test Conf.*, 1985, pp. 785–794.
[7] S. K. Jain and V. D. Agrawal, "Statistical fault analysis," *IEEE Design & Test of Computers*, vol. 2, pp. 38–44, Feb. 1985.
[8] S. C. Seth, L. Pan, and V. D. Agrawal, "PREDICT—Probabilistic estimation of digital circuit testability," in *Proc. 15th Int. Symp. Fault-Tolerant Computing*, 1985, pp. 220–225.
[9] H.-J. Wunderlich, "PROTEST: A tool for probabilistic testability analysis," in *Proc. 22th Design Automation Conf.*, 1985, pp. 204–211.
[10] V. D. Agrawal and S. C. Seth, *Tutorial: Test Generation for VLSI Chips*. Los Alamitos, CA: IEEE Computer Society Press, 1988.
[11] J. E. Stephenson and J. Grason, "A testability measure for register transfer level digital circuits," in *Proc. 6th Int. Symp. Fault-Tolerant Computing*, 1976, pp. 101–107.
[12] L. H. Goldstein, "Controllability/observability analysis of digital circuits," *IEEE Trans. Circuits Syst.*, vol. CAS-26, pp. 685–693, Sept. 1979.
[13] "Will testability analysis replace fault simulation?," Panel discussion, in *Proc. Int. Test Conf.*, 1984, pp. 718–728.
[14] J. Savir, "Improved cutting algorithm," *IBM J. Research and Development*, vol. 34, pp. 381–388, Mar./May 1990.
[15] P. Goel, "Test generation costs analysis and projections," in *Proc. 17th Design Automation Conf.*, 1980, pp. 77–84.
[16] J. Savir, Personal communication.
[17] C. H. Chen and P. R. Menon, "An approach to functional level testability analysis," in *Proc. Int. Test Conf.*, 1989, pp. 373-380.
[18] C. Chen, C. Wu, and D. G. Saab, "Beta: Behavioral testability analysis," in *Proc. Int. Conf. Computer-Aided Design*, 1991, pp. 202–205.

Adaptive Sliding Mode Coordinated Control of Multiple Robot Arms Attached to a Constrained Object

Chun-Yi Su and Yury Stepanenko

***Abstract*— When a common object, attached to multiple robot arms, is cooperatively manipulated to move along a constrained surface, the control task requires the simultaneous control of the motion trajectory of the attached object on the constrained surface; the constrained force due to the contact with the surface; and the internal force exerted by the arms on the object. To accomplish such a control objective, an adaptive sliding mode control algorithm is presented by developing a new concise dynamic model of the system and exploiting its particular properties. Detailed analysis on the tracking properties of the object's position, the constrained force, and the internal force are given. The stability analysis shows that the proposed algorithm can achieve satisfactory tracking performance.**

I. Introduction

In recent years, the coordinated control of multiple robotic manipulators has been investigated by many researchers [1]–[10]. The potential applications of such a system cover a wide range; for example, material handling and assembly, grasping and manipulation

Manuscript received September 5, 1992; revised July 10, 1994. This work was supported by the Natural Science and Engineering Research Council of Canada, the Institute for Robotic and Intelligent Systems (IRIS) and Precarn Associates Inc.

The authors are with the Department of Mechanical Engineering, University of Victoria, Victoria, British Columbia V8W 3P6, Canada.

IEEE Log Number 9409231.

0018-9472/95$04.00 © 1995 IEEE

by a multi-fingered robot hand, and all other tasks recognized to be beyond the capability of a single arm. When multiple robots attach to and manipulate a common object cooperatively, the multiple manipulators, together with the attached object, form a closed kinematical chain. In such a situation, the multiple manipulators are kinematically and dynamically constrained, and the resulting dynamic equations are extremely nonlinear and coupled. The control of such a system becomes more complicated since a set of holonomic equality constraints are imposed and the number of actuators available exceeds the mobility of the system. Thus, the control objective is not only the motion of the manipulated object but also the internal force exerted on the object by the arms, which does not affect its motion.

A number of methods have been proposed for solving this problem [1]–[10]. These methods can be classified in two categories: i) master/slave method [1]–[3], where one or a group of robot arms play the role of the master, and the rest of the arms form the slave group which are moved in conjunction with the master arm(s); ii) hybrid position/force control method [4]–[5], where the position of the object is controlled in certain directions of the workspace, and the force is controlled in the other directions. Each robot arm is controlled using both position and force error.

In addition to the above research efforts, most researches on the coordinated control of two or more robotic manipulators have concentrated on the problem in free space, ignoring the presence of the environment in the workspace. In a variety of tasks, such as bolt assembly or line draw, however, the motion of the object is constrained in some directions due to interaction between the attached object and the environment. In such a case, in addition to the control of the motion of the object and the internal force it is often necessary to control the contact force between the environment and the attached object.

When the environment is modelled as a rigid frictionless constraint surface, a kinematic constraint is imposed on the attached object. This has been extensively studied in recent years for a single arm [11]–[14], and is referred to as nonlinear singular systems [11]. For multiple manipulators the control problem becomes even further complicated, since we have to control simultaneously the motion of the attached object on the constrained surface, the contact force between the attached object and the constrained surface, and the internal force exerted on the object by the arms.

The study of control of the constrained object attached to multiple robots was an open problem until recent efforts described in [15]–[19]. By using the linearizable method, Yun [15], Yoshikawa and Zheng [17] respectively developed their schemes. Cole [16] also proposed a computed torque control method. But it should be noted that the success of the aforementioned schemes relies on the full knowledge of the complex dynamics of the multi-arm system. Care should therefore be taken if there is uncertainty about the system dynamics, as the controller so designed may give degraded performance and may incur instability. To deal with the uncertainties in the dynamics, Hu and Goldenberg [18] proposed an adaptive control law based on the Popov hyperstability theory. But their controller needs the measurements of acceleration and force derivative. Very recently, Yao *et al.* [19] proposed a sliding mode control scheme for a two-arm model. However, the derivation is only based on a simplified model, neglecting the shape of the object.

In this paper, an adaptive sliding mode algorithm for coordinating multiple robot arms is proposed, such that the multi-arm attaches to a common object and moves it along a rigid constrained surface while maintaining a desirable contact force. To do this, firstly, a concise dynamic model of attached object in the object coordinate space is proposed. Then, by recognizing that the degrees of freedom of the generalized coordination decrease while the attached object is constrained, a reduced dynamic model suitable for motion and constraint force control is derived. By exploiting the particular structure of this dynamic model, some fundamental properties are obtained to facilitate controller design. Based on this reduced dynamic model, an adaptive sliding mode controller, using only positions, velocities, and force signals, is proposed. Stability analysis shows the asymptotical tracking of position, contact force, and internal force without requiring any knowledge of the dynamic model.

The organization of this article is as follows: In Section II, the robot dynamics and its structure properties, in the generalized coordinate space of attached object system, are derived. In Section III, a reduced model suitable for control purposes is proposed, and based on this model an adaptive sliding mode control algorithm is proposed. In Section IV some conclusions are presented.

II. System Dynamic Equation Formulation

Although several authors [15]–[19] have proposed a variety of dynamic models for a multi-arm system, in this section we take a different point of view, by combining dynamic equations of n nonredundant arms with that of a rigid attached object, constrained by a rigid surface, to formulate a complete multi-arm model. This model will then be used to develop a sliding mode coordinated control law in Section III.

Consider n robot arms holding a rigid object as shown in Fig. 1, in which all robot end-effectors hold the same object moving along a rigid surface in a coordinated fashion. Define the coordinate system as follows:

O_r: Inertial reference frame.

O_o: Object coordinate frame fixed at the mass center of the object.

O_s: Constraint coordinate frame fixed at the contact point on the object surface.

O_{ai} : ith arm coordinate frame fixed at the ith end-effector located at the grasping point.

We also use notations defined as follows.

$r_o \in R^3$: Position vector of the origin of the frame O_r to the centroid of the object O_o.

$R_o \in R^{3\times 3}$: Orientation of O_o.

$w_o \in R^3$: Angular velocity vector of the object.

$r_i \in R^3$: Position vector from the origin of the frame O_r to the origin of the ith end-effector frame O_{ai}.

$w_i \in R^3$: Angular velocity vector of the arm coordinate system.

$p_i \in R^3$: Position vector of the origin of the object frame O_o to the origin of the frame O_{ai}.

$f_i \in R^3$: Force applied to the object through the attaching point by the ith arm.

$n_i \in R^3$: Moment applied to the object through the attaching point by the ith arm.

M: Mass of the object.

I: Intertial tensor of the object represented by the frame O_o.

To facilitate the dynamic formulation, the following assumptions are made.

A1: Each manipulator is nonredundant, hence all manipulators have the same number of joints.

A2: All the end-effectors of the manipulators are rigidly attached to the common object so that no relative motion occurs between the object and any end-effector.

It should be noted that if rolling and sliding contacts exist between the object and any end-effector [25], [26], the problem will become even more complicated, due to the existence of nonholonomic constraints. This problem, however, is beyond the scope of our discussion in this paper.

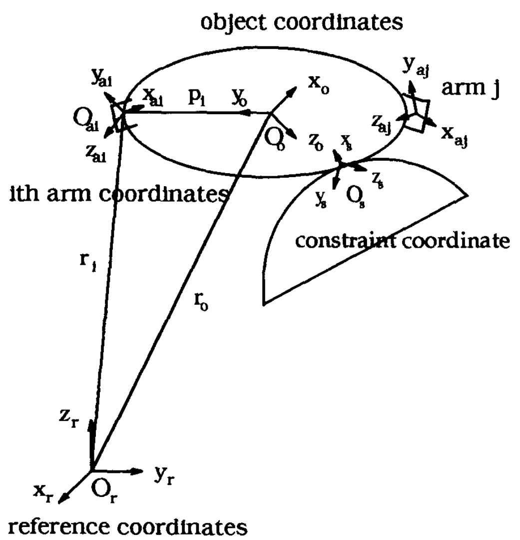

Fig. 1. Coordinate system.

A. Object Dynamics

For simplicity, it is assumed that each contact point is fixed and has a known location on the object. Each robot applies a force f_i and a moment n_i through the contact point C_i to the object. There are in total n ($n \geq 2$) robots acting on the same payload. Firstly, we consider the situation where the environmental constraints on the object are not taken into account. In this case the motion equation of the object manipulated by robot arms is expressed as follows:

$$M\ddot{r}_o = F_o + Mg \tag{1}$$

$$I\dot{w}_o + w_o \times (Iw_o) = N_o \tag{2}$$

where F_o and N_o are the resultant force and moment of the external forces and moments, respectively, applied to the object by robot arms.

$$F_o = \sum_{i=1}^{n} f_i \tag{3}$$

$$N_o = \sum_{i=1}^{n} (n_i + (R_o p_i) \times f_i) \tag{4}$$

where f_i and n_i are the equivalent forces and moments, respectively, applied to the object by the ith arm. Equations (3) and (4) can be rewritten as

$$\begin{bmatrix} F_o \\ N_o \end{bmatrix} = W_1 F_1 + W_2 F_2 + \cdots + W_n F_n \triangleq WF \tag{5}$$

where

$$W_i = \begin{bmatrix} E_3 & 0 \\ (R_o p_i)\times & E_3 \end{bmatrix}, \quad F_i = \begin{bmatrix} f_i \\ n_i \end{bmatrix};$$
$$W = [W_1 W_2 \cdots W_n] \in R^{6\times 6n}, \quad \text{and}$$
$$F = [F_1^T F_2^T \cdots F_n^T]^T \in R^{6n}.$$

In general, the position and orientation of the object are of interest. By using the position and orientation of the object, denoted by $X_o = [r_o^T \;\; \phi_o^T]^T$, where orientation ϕ_o can be expressed as Euler angles, roll-pitch-yaw-angles, or in any other manner, then the expression of (1) and (2) is

$$\begin{bmatrix} ME_3 & 0 \\ 0 & IT_o \end{bmatrix} \ddot{X}_o + \begin{bmatrix} 0 & 0 \\ 0 & w_o \times IT_o + I\dot{T}_o \end{bmatrix} \dot{X}_o + \begin{bmatrix} Mg \\ 0 \end{bmatrix} = WF \tag{6}$$

where T_o is transform matrix and expressed as $w_o = T_o \dot{\phi}_o$.

It should be noted that if Euler angles (ϕ, θ, ψ) are used for ϕ_o, T_o is given by [17]

$$T_o = \begin{bmatrix} 0 & -S_\phi & C_\phi S_\theta \\ 0 & C_\phi & S_\phi S_\theta \\ 1 & 0 & C_\theta \end{bmatrix}$$

where $S_\phi = \sin(\phi), C_\phi = \cos(\phi)$, etc.

Consider now a point C on the object is constrained to follow a physical surface. Supposing the constraints imposed are described by a holonomic smooth manifold, then the algebraic equation for the constraint can be written in the contact point $X_c = [r_c^T, \theta_c^T]^T$ as

$$\Phi(X_c) = 0 \tag{7}$$

where the mapping $\Phi : R^6 \to R^r$ is twice continuously differentiable.

Since $\Phi(X_c) = 0$ is identically satisfied, it is evident that $J_c \dot{X}_c = 0$, where $J_c = \partial\Phi/\partial X_c$ is the Jacobian matrix. Thus, the effect of the constraints on the object can be viewed as restricting the object dynamics to the manifold Ω defined by

$$\Omega = \{(X_c, \dot{X}_c) : \Phi(X_c) = 0; J_c \dot{X}_c = 0\}$$

rather than the space R^{12}.

When the object is moving along the constrained surface, there exists a constraint force $f_c \in R^6$ on the object. Since the constraint surface is frictionless, the constraint force f_c is normal to the constraint surface and we can write

$$f_c = J_c^T \lambda \tag{8}$$

where $\lambda \in R^r$ is the associated Lagrangian multiplier [11].

The constraint force f_c at contact point between the object and constraint surface will produce a resultant force/moment F_c at the object center of mass, given by

$$F_c = S_o^T T^{-T} f_c \tag{9}$$

where

$$S_o = \begin{bmatrix} E_3 & -(R_o p_o)\times \\ 0 & E_3 \end{bmatrix}$$

$p_o \in R^3$ is the vector of the position of the contact point relative to the object frame O_o.

Since the position of frame O_s relative to the frame O_r is given by the expression $r_o + R_o p_o$, the relation between X_o and X_c can be expressed as [16]

$$X_c = \begin{bmatrix} r_o + R_o p_o \\ \phi_o + \text{constant} \end{bmatrix} \triangleq H(X_o) \tag{10}$$

which is known.

Then, based on (6) the dynamic equation of the object, taking into account the environmental constraint, can be expressed as

$$\begin{bmatrix} ME_3 & 0 \\ 0 & IT_o \end{bmatrix} \ddot{X}_o + \begin{bmatrix} 0 & 0 \\ 0 & w_o \times IT_o + I\dot{T}_o \end{bmatrix} \dot{X}_o + \begin{bmatrix} Mg \\ 0 \end{bmatrix} = WF + F_c \tag{11}$$

$$\Phi(H(X_o)) = 0. \tag{12}$$

B. Kinematic Constraints on the Attached Object

At each attaching point C_i, the following kinematic constraint relation between the position r_o and r_i holds

$$r_i = r_o + R_o p_i. \tag{13}$$

Differentiating the above with respect to time yields

$$\dot{r}_i = \dot{r}_o + w_o \times R_o p_i \tag{14}$$

where $w_o \times R = \dot{R}$. Hence, at the attaching point C_i, the following relation can be established.

$$\begin{bmatrix} \dot{r}_i \\ w_i \end{bmatrix} = \begin{bmatrix} E_3 & -(R_o p_i)\times \\ 0 & E_3 \end{bmatrix} \begin{bmatrix} \dot{r}_o \\ w_o \end{bmatrix} \triangleq s_i \begin{bmatrix} \dot{r}_o \\ w_o \end{bmatrix}. \tag{15}$$

Let the position and orientation of the end-effector of the ith arm at attaching point C_i be denoted by $P_i = [r_i^T o_i^T]^T$, the velocity including orientational elements by $v_i = [\dot{r}_i^T, w_i^T]^T \in R^6$, and the joint variable vector by $q_i \in R^6$. Then,

$$v_i = J_i \dot{q}_i \tag{16}$$

where J_i is the generalized Jacobian matrix. Using the (15), it can be shown that

$$s_i \begin{bmatrix} \dot{r}_o \\ w_o \end{bmatrix} = J_i \dot{q}_i. \tag{17}$$

It is assumed in the following, that each robot works in a nonsingular region. Thus the inverse of the matrix J_i exists.

Considering all the robots acting on the object at the same time, the following kinematic constraints are obtained

$$J\dot{\boldsymbol{q}} = S \begin{bmatrix} \dot{r}_o \\ w_o \end{bmatrix} = ST\dot{X}_o \tag{18}$$

where $J = \mathrm{block\,diag}(J_1 \cdots J_n) \in R^{6n\times 6n}, \boldsymbol{q} = [q_1^T \cdots q_n^T]^T \in R^{6n}, S = [s_1^T \cdots s_n^T]^T \in R^{6n\times 6}, T = \mathrm{block\,diag}(E_3 \quad T_o) \in R^{6\times 6}$.

Concerning the matrices W in (5) and S in (18), the following useful properties hold.

Property 2.1:

1) S and W are full rank, i.e., $\mathrm{rank}(W) = \mathrm{rank}(S) = 6$.
2) $S^T = W$.

C. The Combined Robots/Object Dynamics

We now derive the dynamic equation for the whole system in terms of the object variable X_o. If the object moves along the constraint surface in response to manipulation by the multiple arms, it has been shown that the dynamics of the ith robot reflecting object effects is given by

$$D_i(q_i)\ddot{q}_i + B_i(q_i, \dot{q}_i)\dot{q}_i + G(q_i) = u_i - J_i^T F_i, i = 1 \cdots n \tag{19}$$

where $q_i \in R^6$ is the vector of the joint positions; $D_i \in R^{6\times 6}$ is the symmetric, bounded, positive definite inertia matrix; vector $B_i(q_i, \dot{q}_i)\dot{q}_i \in R^6$ presents the centripetal and Coriolis torques; $G(q_i) \in R^6$ is the vector of gravitational torques, which is bounded C^1 function; $u_i \in R^6$ is the vector of applied joint torques, $F_i \in R^6$ is the vector of forces and moments exerted by the ith end-effector on the object defined in (5).

For simplicity, let

$$D = \mathrm{block\,diag}(D_1 \cdots D_n) \in R^{6n\times 6n}$$
$$B = \mathrm{block\,diag}(B_1 \cdots B_n) \in R^{6n\times 6n}$$
$$G = [G_1^T \cdots G_n^T]^T \in R^{6n}$$
$$u = [u_1^T \cdots u_n^T]^T \in R^{6n}.$$

Equation (19) can be expressed more concisely as

$$D(\boldsymbol{q})\ddot{\boldsymbol{q}} + B(\boldsymbol{q}, \dot{\boldsymbol{q}})\dot{\boldsymbol{q}} + G(\boldsymbol{q}) = \boldsymbol{u} - J^T F \tag{20}$$

where $\boldsymbol{q} \in R^{6n}$ is defined in (18), $F \in R^{6n}$ is defined in (5).

The robot model (20) is characterized by the following structural properties, which are of importance to our controller design.

Property 2.2:

1) $D(\boldsymbol{q})$ is symmetric positive definite.
2) A suitable definition of $B(q_i, \dot{q}_i)$ makes matrix $(\dot{D}_i - 2B_i)$ skew-symmetric [21]. In such a case, $(\dot{D} - 2B)$ is also skew-symmetric, i.e.,

$$\boldsymbol{x}^T(\dot{D} - 2B)\boldsymbol{x} = 0.$$

3) The matrices D_i, B_i, and G_i are linear in the dynamic parameters of robot i. More specifically, the following decomposition will hold [21]:

$$D_i(q_i)\ddot{v}_i + B_i(q_i, \dot{q}_i)\dot{v}_i + G(q_i) = Y_i(q_i, \dot{q}_i, \dot{v}_i, \ddot{v}_i)\alpha_i$$

where $Y_i(q_i, \dot{q}_i, \dot{v}_i, \ddot{v}_i) \in R^{6\times m}$ are regressor matrices, $\alpha_i \in R^m$ are vectors of dynamic parameters of robot i. Therefore, the individual terms on the left-hand side of (20) are linear in terms of a suitable selected set of equivalent manipulator and load parameters, i.e.,

$$D(\boldsymbol{q})\ddot{\boldsymbol{v}} + B(\boldsymbol{q}, \dot{\boldsymbol{q}})\dot{\boldsymbol{v}} + G(\boldsymbol{q}) = Y(\boldsymbol{q}, \dot{\boldsymbol{q}}, \dot{\boldsymbol{v}}, \ddot{\boldsymbol{v}})\alpha$$

where $Y(\boldsymbol{q}, \dot{\boldsymbol{q}}, \ddot{\boldsymbol{q}}) \in R^{6n\times m}$ is a regressor matrix of known function of $\boldsymbol{q}, \dot{\boldsymbol{q}}, \ddot{\boldsymbol{q}}$, and $\alpha^T = [\alpha_1, \cdots, \alpha_n] \in R^{(n\times m)}$ is a vector of equivalent parameters.

It is worth noting that there are in total $(6n+1)$ position variables in the (11), (12), and (20), but in fact, only 6 of the variables are independent. This can be easily seen since once the trajectory of the object is given, the joint trajectory of each robot is uniquely determined due to the assumption A1 and A2. Owing to the dependence among position variables, the (11), (12), and (20) would not be suitable for one to analyze the dynamic behavior of this system. With this observation in mind, we will treat elements of the object coordinate X_o as independent position variable and reformulate the dynamic (20) in terms of these variables so as to describe the whole system behavior.

In review of (18) and noting that $w_o = T_o\dot{o}_o$, it is readily obtained that

$$\dot{\boldsymbol{q}} = J^{-1}ST\dot{X}_o \tag{21}$$
$$\ddot{\boldsymbol{q}} = J^{-1}ST\ddot{X}_o + \frac{d}{dt}(J^{-1}ST)\dot{X}_o. \tag{22}$$

With these relations, the dynamic model of the multi-robot system (20) can be reformulated, in terms of the object coordinate X_o, as

$$DJ^{-1}ST\ddot{X}_o + D\frac{d}{dt}(J^{-1}ST)\dot{X}_o + BJ^{-1}ST\dot{X}_o + G(X_o) = \boldsymbol{u} - J^T F. \tag{23}$$

Premultiplying both sides of (23) by $T^T WJ^{-T}$ and using Property 2.1, then, the dynamics model of the multi-robot system, coupled with the object dynamics (11), is

$$D_o(X_o)\ddot{X}_o + B_o(X_o, \dot{X}_o)\dot{X}_o + G_o(X_o) = \boldsymbol{u}_o + T^T S_o^T T^{-T} J_c^T \lambda \tag{24}$$

$$\Phi(H(X_o)) = 0 \tag{25}$$

where

$$D_o = T^T S^T J^{-T} D J^{-1} ST + \begin{bmatrix} ME_3 & 0 \\ 0 & T_o^T I T_o \end{bmatrix}$$

$$B_o = T^T S^T J^{-T} D \frac{d}{dt}(J^{-1}ST) + T^T S^T J^{-T} BJ^{-1} ST + \begin{bmatrix} 0 & 0 \\ 0 & T_o^T w_o \times IT_o + T_o^T I\dot{T}_o \end{bmatrix}$$

$$G_o = T^T S^T J^{-T} G + \begin{bmatrix} Mg \\ 0 \end{bmatrix}$$

$$\boldsymbol{u}_o = T^T W J^{-T} \boldsymbol{u}.$$

The system dynamic equation is now in the general form. It should be noted that the differential-algebraic (23), (24), and (25) completely characterize the dynamic behavior of the multi-arm system. This can be easily observed from the following procedure: by resolving the differential algebraic (24) and (25), we can first obtain the object trajectory X_o and the contact force acting on the constraint surface. Hence, the joint trajectories of each robot are determined through the (18). The evolution of the attached force $F_i, i = 1 \cdots n$, can then be obtained from the (23).

For this system the following properties are found to be true.

Property 2.3

1) D_o is symmetric positive definite.
2) $(d/dt)D_o - 2B_o$ is skew-symmetric.
3)

$$D_o(X_o)\ddot{\boldsymbol{v}} + B_o(X_o, \dot{X}_o)\dot{\boldsymbol{v}} + G_o(X_o) = Y_o(X_o, \dot{X}_o, \dot{\boldsymbol{v}}, \ddot{\boldsymbol{v}})\alpha_o$$

where $Y_o(X_o, \dot{X}_o, \dot{\boldsymbol{v}}, \ddot{\boldsymbol{v}}) \in R^{6\times m}$ is a known regressor matrix, $\alpha_o \in R^m$ is a vector of unknown parameters.

III. The Control Algorithm

The system dynamic (24) and (25) are now in general form which allow development of the control algorithm. The control objective is to provide a set of input joint torques to the end-effectors. These end-effectors attach to the object so that the attached object tracks a desired trajectory on the constrained surface with a specified contact force, at the same time maintaining the desired internal forces exerted on the object.

A. Reduced Dynamic Model

Since the presence of r constraints (25) causes the manipulator to lose r degree of freedom, the motion of the object is left with only $6 - r$ degree of freedom. In this case, $6 - r$ linearly independent coordinates are sufficient to characterize the constrained motion of the object. Choosing $6 - r$ out of 6 object variables, denoted by

$$X_o^1 = [X_o^1 \cdots (X_o^1)_{6-r}]^T \tag{26}$$

to be the generalized coordinates describes the constrained motion of the object. The remaining joint variables are denoted by

$$X_o^2 = [X_o^1 \cdots (X_o^2)_r]^T. \tag{27}$$

By the implicit function theorem, the constraint (25) can always be expressed explicitly as [11]

$$X_o^2 = \sigma(X_o^1). \tag{28}$$

It is assumed that the elements of X_o^1 are chosen to be the first $6-r$ components of X_o. If this is not the case, (24) can always be reordered so that the first $6 - r$ equation correspond to X_o^1 and the last r equation to X_o^2. Defining

$$L(X_o^1) = \begin{bmatrix} I_{6-r} \\ \dfrac{\partial\sigma(X_o^1)}{\partial X_o^1} \end{bmatrix}. \tag{29}$$

Then, from (29)

$$\dot{X}_o = L(X_o^1)\dot{X}_o^1 \tag{30}$$

$$\ddot{X}_o = L(X_o^1)\ddot{X}_o^1 + \dot{L}(X_o^1)\dot{X}_o^1. \tag{31}$$

Therefore, the dynamic model (24), which is restricting to the constraint surface, can be expressed in a reduced form as

$$D_o(X_o^1)L(X_o^1)\ddot{X}_o^1 + B_o^1(X_o^1, \dot{X}_o^1)\dot{X}_o^1 + G_o(X_o^1) = \boldsymbol{u}_o + T^T S_o^T T^{-T} J_c^T \lambda \tag{32}$$

where B_o^1 is defined as

$$B_o^1(X_o^1, \dot{X}_o^1) = D_o(X_o^1)\dot{L}(X_o^1) + B_o(X_o^1, \dot{X}_o^1)L(X_o^1).$$

Remark: Equation (32) is suitable for control purposes which forms the basis for the subsequent development. This is because the quality constraint equation are embedded into the dynamic equation, resulting in an affine nonlinear system without the constraints.

By exploiting the structure of the (32), three properties can be obtained.

Property 3.1: Define the matrix

$$A(X_o^1) = L^T(X_o^1)D_o(X_o^1)L(X_o^1),$$

then

$$\dot{A}(X_o^1) - 2L^T(X_o^1)B_o^1(X_o^1, \dot{X}_o^1)$$

is skew-symmetric.

Proof:

$$\dot{A} - 2L^T B_o^1 = \dot{L} D_o L + L^T \dot{D}_o L + L^T D_o \dot{L} - 2L^T B_o^1 = L^T(\dot{D}_o - 2B_o)L.$$

From Theorem 2.1 that $\dot{D}_o - 2B_o$ is skew-symmetric, it is easy to know that $\dot{A} - 2L^T B_o^1$is also skew-symmetric. ∇.

Property 3.2:

$$J_c T^{-1} S_o T L = L^T T^T S_o^T T^{-T} J_c^T = 0.$$

Proof: Based on the (7), we have

$$\frac{\partial\Phi}{\partial X_c}\frac{dH(X_o)}{dt} = 0. \tag{33}$$

By using (10), $dH(X_o)/dt$ can be expressed as

$$\frac{dH(X_o)}{dt} = T^{-1} S_o T \dot{X}_o.$$

From (30), (33) becomes

$$J_c T^{-1} S_o T L(X_o^1)\dot{X}_o^1 = 0$$

Since X_o^1 is linearly independent, therefore, we obtain

$$J_c T^{-1} S_o T L = L^T T^T S_o^T T^{-T} J_c^T = 0. \qquad \nabla.$$

Property 3.3: Motion (32) is still linear in terms of a suitably selected set of parameters, i.e.,

$$D_o(X_o^1)L(X_o^1)\ddot{\boldsymbol{v}}_o^1 + B_o^1(X_o^1, \dot{X}_o^1)\dot{\boldsymbol{v}}_o^1 + G_o(X_o^1) = Y_1(X_o^1, \dot{X}_o^1, \dot{\boldsymbol{v}}_0^1, \ddot{\boldsymbol{v}}_o^1)\alpha_o. \tag{34}$$

This property can be easily proved from Property 2.3.

The above properties are fundamental for designing the adaptive sliding mode laws.

B. Adaptive Sliding Mode Controller

The controller design problem is as follows: given the desired object trajectory X_o^d and desired constraint force f_c^d, or identically desired multiplier λ_d, which satisfy the imposed constraints, i.e., $\Phi(H(X_o^d)) = 0$ and $f_c^d = J_c^T\lambda_d$, to determine a sliding control law such that for all $(X_o, \dot{X}_o) \in \Omega$, that $X_o \to X_o^d$ and $f_c \to f_c^d$ as $t \to \infty$. It should be noted that, since $X_o^2 = \sigma(X_o^1)$, it is only required to find a sliding control law to satisfy $X_o^1 \to X_o^{1d}$ as $t \to \infty$.

Now, we are ready to introduce the sliding mode coordinated control algorithm by borrowing some conceptual development of the sliding mode control scheme proposed in [14]. Defining

$$e_m = X_o^1 - X_o^{1d} \tag{35}$$

$$\dot{X}_o^{1r} = \dot{X}_o^{1d} - \Lambda e_m \tag{36}$$

where e_m is the tracking error; $\dot{X}_o^{1r}$ is the auxiliary trajectory; Λ is tunable positive definite matrix whose eigenvalues are strictly in the right-half complex plane.

Defining α_1 as a constant m-dimensional vector, containing the unknown elements in the suitably selected set of equivalent dynamic parameters, then the linear parametrizability of the dynamics (Property 3.3) leads to

$$\begin{aligned} D_o(X_o^1)L(X_o^1)\ddot{X}_o^{1r} + B_o^1(X_o^1, \dot{X}_o^1)\dot{X}_o^{1r} + G_o(X_o^1) \\ = Y_1(X_o^1, \dot{X}_o^1, \dot{X}_o^{1r}, \ddot{X}_o^{1r})\alpha_o \end{aligned} \tag{37}$$

where $Y_1(X_o^1, \dot{X}_o^1, \dot{X}_o^{1r}, \ddot{X}_o^{1r})$ is a $6 \times m$ regressor matrix of known function of $X_o^1, \dot{X}_o^1, \dot{X}_o^{1r}, \ddot{X}_o^{1r}$.

The sliding surface is chosen as

$$s_1 = \dot{X}_o^1 - \dot{X}_o^{1r} = \dot{e}_m + \Lambda e_m. \tag{38}$$

The adaptive sliding mode control law is defined as

$$\begin{aligned} \boldsymbol{u}_o = {} & Y_1(X_o^1, \dot{X}_o^1, \dot{X}_o^{1r}, \ddot{X}_o^{1r})\varphi - K_d L(X_o^1)s_1 \\ & - T^T S_o^T T^{-T} J_c^T \lambda_c \end{aligned} \tag{39}$$

$$\varphi_i = -\hat{\beta}_i \operatorname{sgn}\left(\sum_{j=1}^{6-r} s_{1j}(L^T Y_1)_{ji}\right); \qquad i = 1, \cdots, m \tag{40}$$

$$\dot{\hat{\beta}}_i = \eta_i \left|\sum_{j=1}^{6-r} s_{1j}(L^T Y_1)_{ji}\right|; \qquad i = 1, \cdots, m \tag{41}$$

where K_d is a positive definite design matrix, $\eta_i > 0$ are arbitrary constants; λ_c is a force control defined by

$$\lambda_c = \lambda_d - K_\lambda e_\lambda. \tag{42}$$

K_λ is an $m \times m$ constant matrix of force control feedback gains,

$$e_\lambda = \lambda - \lambda_d \tag{43}$$

is the force multiplier error.

The following theorem is proposed.

Theorem: Consider an object attached by n robots, each robot having six degrees of freedom. Let a point $P_c = [r_c^T, \theta_c^T]^T$ on the object be constrained to move along a rigid frictionless constraint surface. Then, for the position/orientation X_o, a constraint $\Phi(H(X_o)) = 0$ is imposed. Suppose no robot goes through a singularity and the grasp maintains force closure over the trajectory. For such a system which is modelled in the reduced form (32), *using the control law* (39)–(41), *with the sliding surface $\boldsymbol{s} = 0$ described by* (38), *the closed-loop system is then globally asymptotically stable in the sense that*

1) *$X_o \to X_o^d$ as $t \to \infty$*
2) *stead-state force $F_c - F_c^d$ is bounded and inversely proportional to the norm of the matrix $(K_\lambda + I)$.*

Proof: The following sliding mode equation can be easily obtained by using (39) and (37)

$$\begin{aligned} D_o L\dot{s}_1 &= D_o L\ddot{X}_o^1 - D_o L\ddot{X}_o^{1r} \\ &= \boldsymbol{u}_o + T^T S_o^T T^{-T} J_c^T \lambda - D_o L\ddot{X}_o^{1r} - B_o^1 \dot{X}_o^{1r} \\ &\quad - G_o - B_o^1 s_1 \\ &= Y_1\varphi - Y_1\alpha_o - B_o^1 s_1 - K_d L(X_o^1)s_1 \\ &\quad + T^T S_o^T T^{-T} J_c^T(\lambda - \lambda_c). \end{aligned} \tag{44}$$

Using the Property 3.2, the above equation becomes

$$A\dot{s}_1 = L^T Y_1\varphi - L^T Y_1\alpha_1 - L^T B_o^1 s_1 - L^T K_d L(X_o^1)s_1. \tag{45}$$

Consider the Lyapunov function

$$V(t) = \tfrac{1}{2}s_1^T A s_1 + \tfrac{1}{2}\sum_{i=1}^{m}(\beta_i - \hat{\beta}_i)^2/\eta_i \tag{46}$$

where $\beta_i = |\alpha_{oi}|$, α_{oi} is defined in (37), $\hat{\beta}_i$ is its estimate.

Differentiating (46) with respect to time along the solution of (45) gives

$$\begin{aligned} \dot{V} = {} & s_1^T(L^T Y_1\varphi - L^T Y_1\alpha_o - L^T B_o^1 s_1 - L^T K_d L(X_o^1)s_1) \\ & + \frac{1}{2}s_1^T\left(\frac{d}{dt}A\right)s_1 + \sum_{i=1}^{m}(\beta_i - \hat{\beta}_i)(-\dot{\hat{\beta}}_i) \Big/ \eta_i. \end{aligned} \tag{47}$$

Using the Property 3.1, (47) becomes

$$\begin{aligned} \dot{V} &= s_1^T(L^T Y_1\varphi - L^T Y_1\alpha_o - L^T K_d L(X_o^1)s_1) \\ &\quad + \sum_{i=1}^{m}(\beta_i - \hat{\beta}_i)(-\dot{\hat{\beta}}_i)/\eta_i \\ &\le -s_1^T L^T K_d L(X_o^1)s_1 - \sum_{i=1}^{m}\beta_i\left|\sum_{j=1}^{6-r} s_{1j}(L^T Y_1)_{ji}\right| \\ &\quad - \sum_{i=1}^{m}\alpha_i\sum_{j=1}^{6-r} s_{1j}(L^T Y_1)_{ji} \\ &\le -s_1^T L^T K_d L s_1 \le 0 \end{aligned} \tag{48}$$

from (46) and (48), it is evident that $||s_1||$ and $\hat{\beta}_i, i = 1, \cdots, m$, are globally bounded. Moreover, $s_1 \to 0$ as $t \to \infty$. Using (38) and a standard argument yields that $e_m \to 0$ and $\dot{e}_m \to 0$ as $t \to \infty$. Also $X_o^2 = \sigma(X_o^1)$, which implies $X_o^2 \to X_o^{2d}$ if $X_o^1 \to X_o^{1d}$, therefore, $X_o \to X_o^d$ as $t \to \infty$.

Since $s_1, e_m, \dot{e}_m$, and $\hat{\beta}_i$ are bounded, using (35) and (36) yields that $X_o^1, \dot{X}_o^1, \dot{X}_o^{1r}, \ddot{X}_o^{1r}$ are all bounded. Therefore, all signals on the right side of (44) are bounded and we conclude that $\dot{s}_1$ is bounded. Using (38) and (35) allows us to conclude that $\ddot{X}_o^1$ is bounded. Substituting the control (39) into the reduced order dynamic model (32) and using Property 3.3, we have

$$\begin{aligned} & Y_1(X_o^1, \dot{X}_o^1, \dot{X}_o^{1r}, \ddot{X}_o^{1r})\varphi - K_d L(X_o^1)s_1 - T^T S_o^T T^{-T} J_c^T \lambda_c \\ & + T^T S_o^T T^{-T} J_c^T \lambda = Y_1(X_o^1, \dot{X}_o^1, \dot{X}_o^{1r}, \ddot{X}_o^{1r})\alpha_1 \end{aligned} \tag{49}$$

which can be written as

$$\begin{aligned} \lambda_c - \lambda = {} & (T^T S_o^T T^{-T} J_c^T)^{-1}[Y_1(X_o^1, \dot{X}_o^1, \dot{X}_o^{1r}, \ddot{X}_o^{1r})\alpha_o \\ & - Y_1(X_o^1, \dot{X}_o^1, \dot{X}_o^{1r}, \ddot{X}_o^{1r})\varphi + K_d L(X_o^1)s_1]. \end{aligned} \tag{50}$$

So all signals on the right side of (50) are bounded, and we can write (50) as

$$\lambda_c - \lambda = \xi_o(X_o^1, \dot{X}_o^1, \ddot{X}_o^1, \dot{X}_o^{1r}, \ddot{X}_o^{1r}, \hat{\beta}_i) \tag{51}$$

where ξ_o is a bounded function. Using (35), (36), and (41) again allows (51) to be written as

$$\lambda_c - \lambda = \xi(X_o^1, \dot{X}_o^1, X_o^{1d}, \dot{X}_o^{1d}, \ddot{X}_o^{1d}) \tag{52}$$

where ξ is a bounded function. Substituting the force control given in (43) into (52) yields

$$e_\lambda = (K_\lambda + I)^{-1}\xi \tag{53}$$

where I is the $m \times m$ identity matrix. Thus, e_λ and therefore the force tracking error $F_c - F_c^d$ is bounded and can be adjusted by changing the feedback gain matrix K_λ. ∇.

Remark:

1) The control laws (39)–(41) do not require any knowledge of the detailed description of the model, and no additional assumption is imposed on the system. So the controller is very general and structurally simple as well as computationally fast.
2) The results for force control is similar to the results presented in [13] for a single arm.
3) The method for computing the regressor matrix Y_1 given in (39) was given by several references, such as [23].
4) While assuring the desired behavior, the control law (39) is discontinuous across the sliding surface s_1, which leads to control chattering. Chattering, in general, is highly undesirable in practice, since it involves extremely high control activity, and further, may excite high-frequency dynamics neglected during modelling [20]. This can be remedied by smoothing out the control discontinuities in a boundary layer neighboring the sliding surface. To do this, we replace $\mathrm{sgn}(\cdot)$ by $\mathrm{sat}(\cdot/\varepsilon)$, where ε is boundary layer thickness. It can be proved that this will guarantee the ultimate boundedness of the system to within any neighborhood of the boundary layer [20], [22].

C. Torque Distribution

For tracking purposes a control algorithm in terms of $\boldsymbol{u}$ is required. Fortunately, since W is full rank (Property 2.2), there exits a matrix $W^+ = W^T(WW^T)^{-1}$, such that (note that $\boldsymbol{u}_o = T^T W J^{-T}\boldsymbol{u}$)

$$\boldsymbol{u} = J^T \boldsymbol{u}_{\mathrm{end}} \tag{54}$$

where

$$\boldsymbol{u}_{\mathrm{end}} = W^+ T^{-T} \boldsymbol{u}_o + F_I \tag{55}$$

is the force causing the motion of the object, in which $\boldsymbol{u}_o$ is computed by (39), and F_I represents an internal force vector. Since the only constraint for F_I is that it should lie within the null space of W, it is not unique, and depends on the load distribution among the robot arms. Due to different applications requirements different choices for F_I, therefore, a many torque distribution methods have been proposed [9], [10]. For this paper, the torque distribution method given in [9] can be applied. The reader may refer to [9].

IV. Conclusion

A robust coordination scheme, for cooperatively manipulating a common object to follow a constrained surface with multiple arms, was presented in this paper. The kinematic and dynamic constraints together with the redundancy in actuation make the control of such a system a formidable problem. The main contributions of this paper lie in the establishment of a new dynamic model to describe the constrained object motion, which makes it possible to seek a sliding mode control law. The proposed algorithm guarantees the simultaneous control of the motion of the object on the constrained surface; the constrained force due to the contact with the surface; and internal force exerted by the arms on the object, using only the measurements of joint position, velocity, and constraint force. The object can be of any shape as long as its mass-center is known.

The computational efficiency for realizing the proposed scheme can be improved by off-line computation of the nonlinear regressor matrix using the desired positions and velocities instead of the actual measurements. The method for implementation of such a strategy is discussed in detail in [24] for a single robot. Therefore, the way to extend the proposed scheme is a further research topic. In developing the control strategy, it is assumed that each arm firmly attaches to the object through the attaching point. For some advanced applications, rolling and sliding contacts between the object and some end-effectors may be required. Hence, extension of the results to the rolling or sliding case is also an interesting further research topic.

References

[1] T. J. Tarn and A. K. Bejczy, "Coordinated control of two robot arms," in *Proc. IEEE Int. Conf. Robotics and Automation*, 1986, pp. 1193–1202.

[2] S. Arimoto and F. Miyazaki, "Cooperative motion control of multiple robot arms or fingers," in *Proc. IEEE Int. Conf. Robotics and Automation*, 1986, pp. 1407–1412.

[3] J. Y. S. Luh and Y. F. Zheng, "Constrained relations between two coordinated industrial robots for motion control," *Int. J. of Robotic Research*, vol. 6, no. 3, pp. 60–70, 1987.

[4] S. Hayati, "Hybrid position/force control of multi-arm cooperating robots," in *Proc. IEEE Int. Conf. Robot. Automat.*, 1986, pp. 82–89.

[5] M. Uchiyama and N. Iwasawa, "Hybrid position/position control for coordination of a two-arm robot," in *Proc. IEEE Int. Conf. Robotics and Automation*, 1987, pp. 1242–1247.

[6] Z. Li, P. Hsu, and S. Sastry, "Grasping and coordinated manipulation by a multifingered robot hand," *Int. J. Robotic Research*, vol. 8, no. 4, pp. 33–50, 1987.

[7] J.-H. Jean and L.-C. Fu, "An adaptive coordinated control scheme for multi-manipulator systems" in *Proc. American Control Conference*, 1991, pp. 3050–3054.

[8] M. Koga, K. Kosuge, K. Furuta, and K. Nosaki, "Coordinated motion control of robot arms based on the virtual internal model," *IEEE Trans. Robotics Automat.*, vol. 8, pp. 77–85, 1992.

[9] Y. D. Song and J. N. Anderson, "Adaptive control of a colleague-like multi-robot system handling a common object," in *Proc. IEEE Conf. Decision and Control*, 1991, pp. 2787–2792.

[10] P. Hsu, "Control of multi-manipulator systems-trajectory tracking, load distribution, internal force control, and decentralized architecture," in *Proc. IEEE Int. Conf. Robotics and Automation*, 1989, pp. 1234-1239.

[11] N. H. McClamroch and D. Wang, "Feedback stabilization and tracking of constrained robots," *IEEE Trans. Automat. Contr.*, vol. 33, pp. 419–426, 1988.

[12] C. Y. Su, T. P. Leung, and Q. J. Zhou, "Adaptive control of robot manipulators under constrained motion," in *Proc. IEEE Conf. Decision and Control*, 1990, pp. 2650–2655.

[13] R. Carelli and R. Kelly, "An adaptive impedance/force controller for robot manipulators," *IEEE Trans. Automat. Contr.*, vol. 36, pp. 967–971, 1991.

[14] C. Y. Su, T. P. Leung, and Q. J. Zhou, "Force/motion control of constrained robots using sliding mode," *IEEE Trans. Automat. Contr.*, vol. 37, no. 5, pp. 668–672, 1992.

[15] X. Yun, "Nonlinear feedback control of two manipulators in presence of environmental constraints," in *Proc. IEEE Int. Conf. Robotics and Automation*, 1989, pp. 1252–1257.

[16] A. A. Cole, "Constrained motion of grasped objects by hybrid control," in *Proc. 29th Conf. Decision and Control*, 1990, pp. 1954–1959.

[17] T. Yoshikawa and X. Zheng, "Coordinated dynamic hybrid position/force control for multiple robot manipulators handling one constrained object," in *Proc. IEEE Int. Conf. Robotics and Automation*, 1990, pp. 1178–1183.

[18] Y.-R. Hu and A. A. Goldenberg, "An adaptive approach to motion and force control of multiple coordinated robot arms," in *Proc. IEEE Int. Conf. Robotics and Automation*, 1989, pp. 1091–1096.

[19] B. Yao, W. B. Gao, S. P. Chan, and M. Cheng, "VSC coordinated control of two manipulator arms in the presence of environmental constraints," *IEEE Trans. Automat. Contr.*, vol. 37, pp. 1806–1812, 1992.

[20] J. J. E. Slotine and S. S. Sastry, "Tracking control of nonlinear system using sliding surface, with application to robot manipulators," *Int. J. Control*, vol. 38, pp. 465–492, 1983.

[21] J. J. E. Slotine and W. Li, "On the adaptive control of robot manipulators," *Int J. of Robotics Research*, vol. 6, pp. 49–57, 1987.

[22] F. Esfandiari and H. K. Khalil, "Stability analysis of continuous implementation of variable structure control," *IEEE Trans. Automat. Contr.*, vol. 36, pp. 616–620, 1991.

[23] J. Yuan and Y. Stepanenko, "Computing a manipulator regressor without acceleration feedback," *Robotica*, vol. 10, pp. 269–275, 1992.
[24] Y. Stepanenko and C. Y. Su, "Regressor based sliding mode control of robotic manipulator," in *Proc. 31th IEEE Conf. Decision and Control*, 1992, pp. 1410–1416.
[25] A. A. Cole, J. E. Hauser, and S. S. Sastry, "Kinematics and control of multifingered hands with rolling contact," *IEEE Trans. Automat. Contr.*, vol. 34, pp. 398–404, 1989.
[26] A. A. Cole, P. Hsu, and S. S. Sastry, "Dynamic control of sliding by robot hands for regrasping," *IEEE Trans. Robotics Automat.*, vol. 8, pp. 42–52, 1992.

Teleoperator Response in a Touch Task with Different Display Conditions

Alberto Rovetta, Francesca Cosmi, and Lorenzo Molinari Tosatti

***Abstract*—This paper deals with the evaluation of human biofeedback response in virtual reality and in direct view. The experiments have been performed with a new paradigm for the evaluation of human biofeedback during the telemanipulation performance of a touch task. The controlled motion of one finger is monitored with the surface EMG, while a mechanical robotized hand finger follows the motion imposed by the human finger. The biofeedback is detected in a direct way, by the vision of the robotized finger action, and in an indirect way, with the support of three different types of interfaces. The neuromuscular activity presents different features and delays in the four cases: A measurement of the attention and participation in the man/machine interface is obtained, in a first series of experiments. The paradigm adopted in this research is the result of the integration of robotics and neurology.**

I. Neurobiology and Neurorobotics Project

This paper examines the influence of biofeedback on the muscular strategy by which a motion plan is executed. In telemanipulation, the control of a remote system is performed by a human operator, as part of the telemanipulation control loop. A better understanding of mechanical and manipulating systems control can be achieved by means of a comparative study of biological systems. Hogan has investigated the problem of formalizing informational and energetic transactions in control system software and in physical systems, with application to the problem of contact during telemanipulation [1].

Mechanical informations such as position, pressure distribution, force and so on are required for a better knowledge of human behavior as well as of human kinematics and contact movements, while sensory systems in robotics can provide methods and tools to achieve comfortable man-machine interfaces. Human sensory fusion has been analyzed by means of virtual reality interfaces by Ishikawa [2].

High fidelity real-time computer graphics displays as well as a force reflecting teleoperation simulator have been developed at JPL to provide operator aid in telemanipulation tasks, and different types of interfaces have been evaluated [3], [4].

Manuscript received May 7, 1993, revised April 1, 1994 and July 10, 1994. This work was supported by C.N.R. (Italian National Council of Researches) and M.P.I (Ministry of Education).

The authors are with the Department of Mechanics, Politecnico di Milano, 20133 Milano, Italy.

IEEE Log Number 9409228.

The process of visual search in virtual environments has been investigated by Stark *et al.*, as well as the role of visual depth cues and effects of stereo and occlusion on simulated manipulation [5].

Experimental studies were conducted by Massimino and Sheridan to determine the effects of visual and force feedback on human performance in telemanipulation, with varying frame rates and subtended visual angles, with and without force feedback [6]. Kazerooni has proposed a framework for the design of a telerobot controller in which the dynamic behaviors of master and slave systems are mutually dependent [7]. In his book [8], Sheridan provides a wide survey on the efforts that have been made to model the man-in-the-loop and the operator's role in supervisory control.

Our research provides an experimental evaluation of the different control strategies adopted by the human neuromuscular system when the same teleoperation task is performed with the aid of different man/machine interfaces [9], [10], [11].

The EMG recording during a teleoperation experiment, performed both in conditions of direct visual contact with the remote environment and utilizing different interfaces, allows an investigation of the neuromuscular activity of a human subject. A better understanding of how human control is performed can then be achieved.

The sensory signals processed by the cerebral cortex and the cerebellum represent the feedback aspect in the human control loop. To adjust neuromuscular activity to the desired behavior in anticipation of the sensory signals is performed by a feedforward control as the human motion plan does not contain, in itself, a complete description of the task [12].

In this experiment, the operator wears an exoskeleton system that drives the mechanical finger motion. During the operator's finger motion, the sensed signals from the exoskeleton change and these changes provide signals to actuate the mechanical finger.

The sensory biofeedback in the tests is obtained by the eyes, which are observing the performance of the telemanipulation action and the contact force of the robotic finger, depicted on a monitor or expressed by the bending of a loaded blade. The line-of-sight distances from the operator's eyes to the display and the blade are respectively 2 meters and 1.30 meters.

The process monitoring continues throughout the duration of the test. The following signals are sampled and memorized for quantitative analysis: 1) operator's finger motions, 2) EMG signals, 3) forces exerted by the mechanical finger on the blade.

II. Test Equipment

The test equipment makes use of appropriately integrated mechanical, electronic and display components. The integration itself allowed the development of a system which is able to provide different types of feedback to the operator and to carry out a quantitative analysis of the test execution modes.

The main features of the experimental station are (Fig. 1):

1) Telerobotic hand, a mechanical gripping device with three independent fingers with phalanxes articulation, actuated by three motors which stretch and release a metal tendon, developed in the Robotics Laboratory of the Department of Mechanics, Politecnico di Milano. In this first stage of the experiments, was decided that only one of the fingers should be used, to simplify the execution of the test. Therefore, only one of the mechanical fingers was programmed to accept direct control by the operator. The elements of the experiment include the following: